Electronic Properties of Two Adjacent Intramolecular Hydrogen Bonds and their Effects to the Molecular Charge Distribution: Experimental Synchrotron Microcrystal and DFT Computational Study

Magdalena Małecka*[a], Stefan Mebs*[b], Andrzej Jóźwiak[c]

[a] Department of Structural Chemistry and Crystallography, University of Łódź, Pomorska 163/165, 90-236 Łódź, Poland, E-mail: malecka@uni.lodz.pl

[b] Humboldt Universität zu Berlin, Mathematisch-Naturwissenschaftliche Fakultät I, Institut für Chemie, Anorganische und Allgemeine Chemie I, Brook-Taylor-Str. 2, 12489 Berlin, Deutschland, E-mail: stefan.mebs@chemie.hu-berlin.de

[c] Department of Organic Chemistry, University of Łódź, Tamka 12, 91-403 Łódź, Poland

Abstract

The experimental crystal structure and corresponding theoretical electron density determination of 2-hydroxy-4,4-dimethyl-6-oxo-cyclohex-1-ene carboxy amide is reported with special focus on two adjacent intramolecular hydrogen bonds (O-H...O and N-H...O). The possible tautomeric forms are studied and their theoretical populations in the gas phase were determined. Additionally, theoretical models which refer to the title compound were optimized and investigated in terms of the combined analysis of ED-topology, energy densities, electron localizability indicator (ELI), delocalization index and source function (SF). This analysis confirmed the O-H…O interactions to be resonance assisted and of medium strength, while the N-H…O interactions are rather weak. Moreover, the influence of the intramolecular hydrogen bonds to the delocalization within the six-membered rings is determined. In all cases the hydrogen bond strength and amount of resonance within the six-membered rings is related to the types of interactions (O-H...O and/or N-H...O) and to the molecular symmetry.

1. Introduction

Intramolecular hydrogen bonds and their crucial role in biological chemistry have been reported in the literature [1]. Mostly, intramolecular hydrogen bonds are part of planar six-membered rings stabilized by a conjugated π-system. The structure and electron density determination of the title compound, (I) that includes two adjacent intramolecular hydrogen bonds have been reported. Our research has been recently focused to this topic using experimental and computational methods [2,3]. It turned out that in such systems π-electron delocalization appears in H-bonded rings, which entails a change in the geometrical and

2

topological parameters [4]. Thus, the intramolecular hydrogen bonds were regarded as resonance-assisted hydrogen bonds (RAHB). In this work we focus on systems that exhibit two intramolecular hydrogen bonds in adjacent six-membered rings. How does the presence of two adjacent hydrogen bonds affect the geometrical and topological parameters? The known compound (I) is almost a prototypical example for systems with a O-H…O and a N-H…O hydrogen bond. It was prepared following a synthesis known from literature [5]. A similar moiety of two adjacent strong intramolecular hydrogen bonds was examined by Bertolini [6]. Due to their biological relevance and pharmacological activity series of related compounds with a hydroxy group in *cis* conformation to an amidic moiety were investigated [7,8].

However, the crystal structure of (I) has not been elucidated yet. Unfortunately, only very small crystals were obtained. Because of the weak diffraction, data collection was carried out at the synchrotron beamline F1 at Hasylab/DESY. The crystal structure determination reveals the favored tautomeric form in the crystal lattice and what factors stabilize it. In order to investigate in detail the double intramolecular hydrogen bond formation, six optimized structures of smaller model compounds were compared in terms of Quantum Theory of Atoms in Molecules (QTAIM) [9], Electron Localizability Indicator (ELI) [10], source function (SF) [11], and delocalization index [12].

2. Results and Discussion

2.1. Crystal structure

Compound (I) crystallizes in the monoclinic space group P2$_1$/c. The molecular structure is shown in Fig. 1. The cyclohexene ring (ring 'c') adopts a slightly distorted half-boat conformation with an apical C4 atom. The puckering parameters [13] are: $Q_T =$

0.449(2)Å, $\varphi_2 = 4.2(2)^\circ$, $\theta_2 = 129.0(2)^\circ$. The remaining non-hydrogen atoms in the flat part of the molecule have a maximum deviation from the best plane of 0.076(2) Å for the C5 atom.
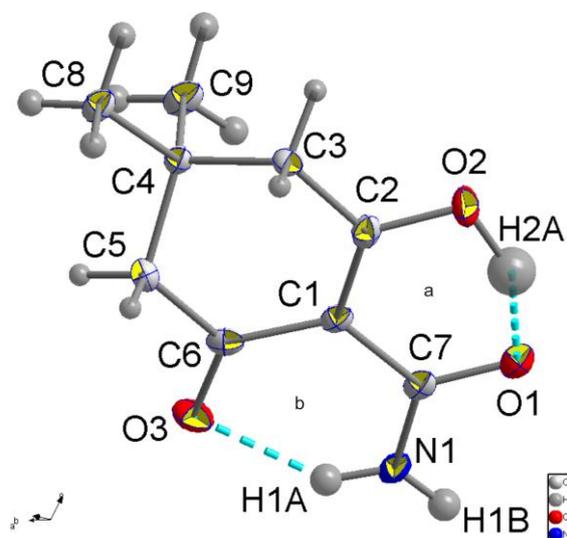
Figure 1 Molecular structure of (I) including the atom numbering scheme. The intramolecular N-H…O and O-H...O hydrogen bonds are displayed as dashed lines. Anisotropic displacement ellipsoids are drawn at 50% probability.

Difference electron-density maps for (I) revealed the position of the H2A atom in the vicinity of atom O2, clearly indicating that the molecule exists in the monoketo-amide form and that the O1 atom of the carbonyl group is involved in an intramolecular resonance-assisted hydrogen bond [14]. The geometry of this hydrogen bond, with long O-H and short H…O distances, together with a large displacement parameter of the H atom, is typical for interactions with a broad shallow energy minimum [15]. Both of the A- and B-tautomeric forms (see Scheme 1) are stabilized by an additional intramolecular hydrogen bond (N1-H1A…O3), however form B is preferred in the crystal structure. Both hydrogen bonds are designated as the S(6) motif according to Etter [16] (Table 1). Short intramolecular O-H…O hydrogen bonds in the vicinity of a second intramolecular N-H…O hydrogen bond have

already been observed and reported for a few structures [17-20]. In addition, an intermolecular hydrogen bond contact (N1-H1B…O1^i) is observed, that links two neighboring molecules by a center of inversion. These two inter-molecular hydrogen bonds represent a common packing motif $R_2^2(8)$ [16]. The crystal packing in the unit cell is presented in Fig. 2.
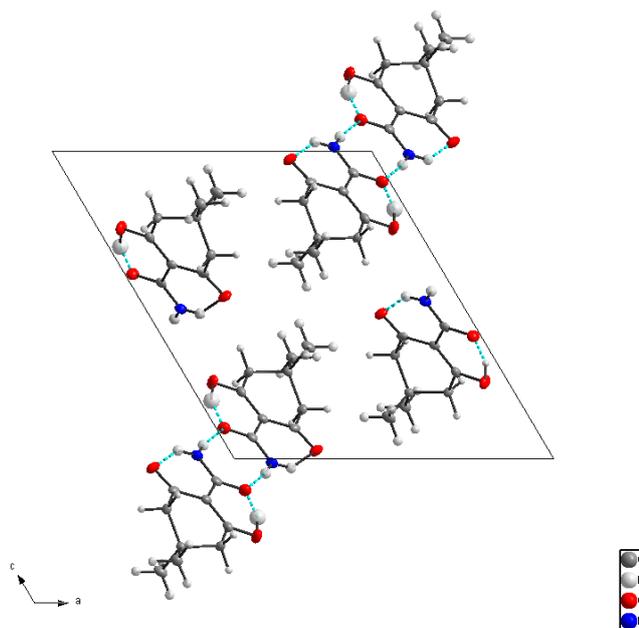
Figure 2 Packing of the molecules displayed along the b direction. The intramolecular and intermolecular hydrogen bonds within dimers are marked as black lines

Table 1. Geometrical (Å, °) data of form B obtained by X-ray diffraction and geometrical and topological (ρ in e/A3, $\nabla^2\rho$ in e/A5) data of form A, B and C and the dimer obtained by theoretical geometry optimization of the gas-phase structures. Hydrogen-bonding energies are calculated according to Espinosa [34] ($E = 25.3 \times 10^3 e^{-3.6(H...A)}$) and $E_{HB} = \frac{1}{2} V(\mathbf{r}_{BCP})$ (in kcal/mol) with local energy densities G, V, H (in a.u.).

	D-H	H...A	D...A	<D-H…A	ρ(H...A)	$\nabla^2\rho$	E_{HB}geom	E_{HB}	G	V	H	V/G
O-H…O												
O2-H2A...O1[#]	1.17(3)	1.37(3)	2.479(1)	153(3)	0.75	1.3	-42.85	-39.49	0.0695	-0.1259	-0.0563	1.80
O2-H2A...O1[$]	1.02	1.55	2.479	150	0.53	3.7	-23.07	-24.08	0.0582	-0.0768	-0.0186	1.32
O2-H2A…O1[&]	1.03	1.51	2.460	151	0.51	3.4	-26.83	-27.51	0.0632	-0.0877	-0.0244	1.38
O2-H2A…O1[*]	1.02	1.52	2.465	151	0.51	3.8	-25.79	-26.57	0.0623	-0.0847	-0.0224	1.35
N-H...O												
N1-H1A...O3[#]	0.88(3)	1.94(2)	2.677(2)	139(2)	0.19	2.8	-5.60	-7.11	0.0269	-0.0227	0.0033	0.84
N1-H1B…O1i[#]	0.86(2)	2.12(2)	2.969(2)	170(2)	0.11	1.7	-2.92	-3.48	0.0141	-0.0113	0.0033	0.80
N1-H1A...O3[$]	1.01	1.96	2.703	128	0.17	2.6	-5.26	-6.33	0.0235	-0.0202	0.0033	0.86
N1-H1A...O3[&]	1.01	1.89	2.683	132	0.19	3.1	-6.67	-7.97	0.0271	-0.0254	0.0016	0.94
N1-H1A...O3[##]	1.01	2.03	2.792	129	0.16	2.1	-4.00	-5.23	0.0191	-0.0167	0.0024	0.87
N1-H1A…O3[*]	1.02	1.89	2.695	133	0.21	2.7	-6.56	-7.0	0.0269	-0.0252	0.0017	0.93
N1-H1B…O1i[*]	1.02	1.92	2.944	175	0.18	2.2	-5.93	-6.15	0.0214	-0.0196	0.0018	0.91

symmetry code (i): 1-x, -y, -z , [#] - form B exp. geom., [$]- form A, [&] -form B, [*]dimer, [##] form C

2.2. Theoretical molecular energies

The energy differences between forms A, B and C (Scheme 1) are given in Table 2 in terms of pure electronic and zero-point-corrected energies and Gibbs free energies.

SCHEME 1. Scheme of compound (I) with its tautomeric forms

form A   form B   form C

The relative populations of the tautomers in the gas phase were estimated using the Boltzmann distribution law. This methodology has been proved to be useful to describe tautomeric equilibria [21, 22]

$$\frac{N_i}{N_j} = \frac{q_1}{q_2} e^{-\frac{E_i - E_j}{k_B T}} \qquad (1)$$

where N is the number of tautomer molecules, q is the partition function for the tautomer, E is the energy corresponding to the tautomer's lowest energy state, k_B is the Boltzmann constant,

and T is the temperature. The combined populations of all three tautomers are assumed to give 100%. The DFT calculations show that the B form is the most stable tautomer in the gas phase as it has a lower energy than forms A and C by 18.6-20.6 kcal/mol, respectively, (Table 2). The contributions of forms A and C in the gas phase of a tautomeric mixture are exceptionally small ($<10^{-10}$%), which confirms the experimental findings.

Table 2. Total energies (in hartree), relative energies (kcal/mol) and populations in % for tautomers A, B, and C of 2-hydroxy-4,4-dimethyl-6-oxo-cyclohex-1-ene carbox amide at the B3LYP/6-311++G** level of approximation.

	E	ΔE_{ZPE}	ΔE	ΔG^{298}	% P_i
form A	-631.4150883	20.3	20.6	20.1	$2 \cdot 10^{-15}$
form B	-631.4479022	0	0	0	100
form C	-631.4183064	18.2	18.6	18.2	$2 \cdot 10^{-13}$

2.3. Molecular Geometries

The differences in the geometric parameters of the three tautomeric structures are listed in Table 3. When form B is transformed into form A a decrease of the C5-C6 distance is observed, with a concomitantly larger O3-C6 bond distance. When form B is transformed into form C the C1-C2 bond is elongated from 1.388 Å to 1.556 Å, the typical distance for a single $C_{sp3} - C_{sp3}$ connection [23], whereas the O2-C2 bond length decreases considerably (1.310 Å to 1.202 Å). The most significant differences between the optimized geometry of form B and the experimental structure are found in the O1-C7 and N1-C7 bonds, where the experimental bond distance of O1-C7 is longer (1.284(2) Å compared to 1.254 Å) and the N1-C7 distance is shorter (1.318(2) Å compared to 1.342 Å). However, these changes could be explained not only by the fact, that molecules form dimers in the crystal lattice, but also by the π-electron

8

delocalization effect within RAHB system, and strengthening of the hydrogen bond (see, Table 1, energy values -42.85 kcal/mol vs. -26.83 kcal/mol). Nevertheless, the large influence on the conjugation in the RAHB system and the strengthening of the resonance assisted hydrogen bonds is a problem for future investigations. Other bond lengths are very similar in the three optimized species and in good agreement with the solid state structure (Table 3).

For the three tautomers a different conformation of the cyclohexene rings is also observed. In tautomer B it adopts a slightly distorted half-boat conformation, with ring-puckering parameters [13] for the atom sequence C1-C6-C5-C4-C3-C2: $Q_T = 0.449(2)$Å, $\varphi_2 = 172.4(2)°$, $\theta_2 = 52.5(2)°$, whereas the remaining cyclohexene rings have the conformation between half-chair and twist-boat in tautomer A and chair conformation in form C. The ring-puckering parameters are: $Q_T=0.407(2)$Å, $\varphi_2=209.3(2)°$, $\theta_2=64.7(2)°$ for tautomer A, and $Q_T=0.575(2)$Å, $\varphi_2=332.6(2)°$, $\theta_2=3.5(2)°$ for tautomer C, (see also Fig. S1).

Table 3. Selected geometrical parameters (first row) [Å] for compound (I), the optimized dimer and three possible tautomers of 2-hydroxy-4,4-dimethyl-6-oxo-cyclohex-1-ene carboxy amide, calculated at the B3LYP/6-311++G** level of theory. Second and third rows refer to the theoretical electron density at the bcp ($\rho(\mathbf{r})$ [e/ Å^3]) and its Laplacian ($\nabla^2\rho(\mathbf{r})$ [e/ Å^5]).

	form B_exp	OPT_dimer	form A	form B_opt	form C
O1-C7	1.284(2)	1.268	1.254	1.254	1.218
	2.40	2.38	2.56	2.55	2.75
	-13.9	-12.9	-11.2	-11.1	-6.7
O2-C2	1.311(2)	1.312	1.319	1.310	1.202
	2.22	2.22	2.16	2.20	2.81
	-10.6	-10.5	-9.1	-8.9	0.2
O3-C6	1.250(2)	1.231	1.385	1.232	1.216
	2.55	2.55	1.82	2.63	2.73
	-7.9	-7.9	-8.5	-5.0	-1.432

|					
N1-C7	1.318(2)	1.330	1.353	1.342	1.354
	2.38	2.38	2.20	2.26	2.19
	-25.3	-25.9	-23.5	-24.1	-23.0
C1-C2	1.400(2)	1.387	1.380	1.388	1.556
	2.07	2.07	2.14	2.16	1.56
	-20.1	-20.1	-21.2	-20.9	-11.61
C1-C6	1.459(2)	1.464	1.472	1.462	1.533
	1.87	1.87	1.81	1.86	1.64
	-16.8	-16.8	-16.1	-16.7	-13.1
C1-C7	1.478(2)	1.482	1.472	1.482	1.535
	1.81	1.81	1.82	1.80	1.65
	-15.9	-15.9	-16.1	-15.9	-13.5
C2-C3	1.504(3)	1.500	1.501	1.500	1.518
	1.73	1.73	1.75	1.76	1.56
	-15.1	-15.1	-15.5	-15.6	-11.6
C3-C4	1.544(2)	1.540	1.543	1.541	1.554
	1.60	1.60	1.61	1.61	1.56
	-12.4	-12.4	-12.6	-12.7	-11.8
C4-C7	1.542(2)	1.537	1.547	1.542	1.537
	1.60	1.60	1.58	1.61	1.56
	-12.3	-12.3	-12.3	-12.6	-12.8
C4-C8	1.539(2)	1.541	1.538	1.537	1.541
	1.60	1.59	1.61	1.61	1.56
	-12.4	-12.4	-12.7	-12.8	-12.6
C4-C5	1.540(2)	1.539	1.518	1.540	1.558
	1.61	1.61	1.66	1.61	1.54
	-12.5	-12.6	-13.6	-12.7	-11.5
C5-C6	1.515(2)	1.522	1.341	1.522	1.514
	1.71	1.70	2.27	1.70	1.54
	-12.6	-12.6	-13.6	-12.7	-11.5

2.4. *Intramolecular hydrogen bonds and comparison with the CSD-database*

In tautomers A and B the same type of hydrogen bonds (N-H…O, and O-H…O) is observed as in the crystal structure. Their geometrical parameters do not differ significantly except for the D-H distance which in the case of the N-H…O hydrogen bond is shorter and in the case of O-H…O hydrogen bond is longer with respect to the values obtained theoretically.

Tautomer C exhibits only one N-H…O hydrogen bond. The longer distances H…A (2.03Å) and D…A (2.792Å) compared to the corresponding values in the tautomers A and B indicate that this hydrogen bond is the weakest of all N-H…O hydrogen bonds in the three tautomers.

A search of the Cambridge Structural database (Version 1.13) [20] for compounds that exhibit two adjacent hydrogen bonds (Scheme 2), yields the structures of 9 related derivatives. The relevant geometrical parameters of the six-membered rings with intramolecular hydrogen bonds are presented in Table 4.

Scheme 2. Two adjacent hydrogen bonds in CSD entry scheme (with abbreviation of distances in the H-bonded rings).
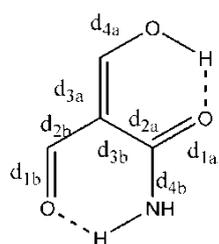
The π-electron delocalization within intramolecular hydrogen bonded systems has consequences for the geometrical parameters of the rings. These changes are larger if the hydrogen bonds are resonance-assisted. Equalizations of the C-C bond lengths d2 and d3 on the one hand and of the C-X bonds (X = O, N) d1 and d4 on the other hand are observed, but are more distinct for the homonuclear O-H...O ring fragment than for the heteronuclear N-H...O ring fragment. This equalization is not complete as the formal C=C double bond d3a remains ca. 0.08 Å shorter compared to the d2a bond. This is in agreement with the structures found in the CSD database. However, the coupling parameter λ proposed by Gilli [25] is

0.484 for the investigated crystal structure. $\lambda = 1, 0$ refers to the keto-enol form, while $\lambda = 0.5$ denotes fully π-delocalization within the hydrogen-bonded ring. For all corresponding structures found in the database λ is in the range between 0.483-0.489. Nevertheless, for the present structure an elongation of the d1a distance by 0.073 Å and a slight shortening of the d4a distance is observed. The movement of the proton causes the shortening of the O…O contact to 2.479.

Table 4. Geometrical parameters [Å, °] for hydrogen bonds and H-bonded rings in the structures that were found in the CSD-database.

First row refers to the intramolecular O-H...O hydrogen bond, the second one refers to the N-H...O hydrogen bond.

refcode	D-H	H...A	D...A	<D-H...A	d1a d1b	d2a d2b	d3a d3b	d4a d4b	λ
AOTETC	0.982	1.553	2.442	148	1.274	1.467	1.397	1.291	0.487
	1.145	1.167	2.670	142	1.228	1.434	1.467	1.334	
ATETCY10	0.986	1.676	2.436	130	1.295	1.443	1.409	1.225	0.488
	0.824	1.996	2.672	143	1.223	1.434	1.443	1.299	
BINNAN	1.210	1.229	2.417	164	1.275	1.461	1.394	1.285	0.487
	0.891	2.034	2.723	133	1.226	1.441	1.461	1.308	
BODWAS	1.126	1.329	2.436	165	1.281	1.460	1.397	1.285	0.489
	0.926	1.987	2.692	131	1.229	1.438	1.460	1.308	
CMTCYH10	1.200	1.362	2.461	147	1.310	1.437	1.429	1.241	0.488
	0.882	2.026	2.711	133	1.224	1.417	1.437	1.311	
DEMXTC10	0.994	1.481	2.431	158	1.78	1.466	1.392	1.304	0.485
	0.862	2.028	2.7222	136	1.236	1.440	1.466	1.317	
DEMXTC20	0.992	1.483	2.431	157	1.278	1.466	1.392	1.305	0.485
	0.856	2.024	2.717	137	1.236	1.439	1.466	1.322	
OXYTET	1.084	1.394	2.429	156	1.274	1.473	1.391	1.304	0.483
	0.872	2.100	2.763	132	1.233	1.438	1.473	1.323	
mean value	1.072(8)	1.438(12)	2.435(10)	154(9)	1.283(10)	1.459(10)	1.400(10)	1.284(2)	0.491
	0.907(9)	1.983(11)	2.709(20)	136	1.229(4)	1.435(6)	1.459(10)	1.315(9)	
form B*	1.17(3)	1.37(3)	2.479	153	1.284(2)	1.478(2)	1.400(2)	1.311(2)	0.484
	0.88(2)	1.94(2)	2.677	139	1.250(2)	1.459(2)	1.478(2)	1.318(2)	
reference [19]					1.210	1.464	1.340	1.333	
					1.210	1.464	1.464	1.336	

[#] - form B exp. geom.

2.5.   *Topological parameters for H-bonded rings*

It was shown in many papers [26-29] that the topological parameters reflect the character of chemical bonding and their strength by using Bader's 'Atoms in Molecules Quantum Theory' (QTAIM), in particular hydrogen bonds [9, 30]. Koch and Popelier [31] proposed eight criteria of the existence of hydrogen bonds based on the electron density $\rho(\mathbf{r})$ at a bond critical bond (bcp) and the Laplacian $\nabla^2\rho(\mathbf{r})$ at the bond critical point (bcp). Additionally, a characteristic behavior is found for the energy denisties: $G(\mathbf{r}_{bcp})$, $V(\mathbf{r}_{bcp})$, $H(\mathbf{r}_{bcp})$, kinetic, potential and total electron energy densities at the bcp. These are related to each other in the following way:

$$\frac{1}{4}\nabla^2\rho(r) = 2G(r_{BCP}) + V(r_{BCP}) \quad (2)$$

$$H(r_{BCP}) = G(r_{BCP}) + V(r_{BCP}) \quad (3)$$

Rozas [32] and coworkers classified hydrogen bonds (hb) on the basis of $\nabla^2\rho(\mathbf{r})$ and $H(\mathbf{r}_{bcp})$ values. They found that weak hydrogen bonds indicate both positive $\nabla^2\rho(\mathbf{r})$ and $H(\mathbf{r}_{bcp})$ values in accordance with dominating electrostatic forces, whereas medium hb show $\nabla^2\rho(\mathbf{r})>0$ and $H(\mathbf{r}_{bcp})<0$. For strong hydrogen bonds both $\nabla^2\rho(\mathbf{r})$ and $H(\mathbf{r}_{bcp})$ are negative ndicating covalent interactions [33].

According to these criteria all intramolecular O-H…O hydrogen bonds in the discussed models (see Scheme 3 and Scheme 1) appear as medium interactions with total $H(\mathbf{r}_{bcp})$ being slightly negative (Table 1 and Table 5). Thus, they can be qualified as partially covalent interaction. The theoretical electron density for the experimental geometry (H…A

contact of 1.37 Å) is $\rho(\mathbf{r}) = 0.75$ e/Å^3 at the bcp; for the optimized geometries smaller values of 0.35 to 0.55 e/Å^3 are found which tend to decrease with increasing H…O lengths. The Laplacian values are positive and small, as it is expected for moderate interactions. The same is true for N-H…O hydrogen bonds in models 13, 23. The remaining N-H…O hydrogen bonds are weak interactions. The electron densities at the correspomding bcps are low, ranging between 0.19 and 0.27 e/Å^3, which corresponds to the electrostatic character of these interactions.

Scheme 3. Scheme of the optimized models. The last row shows a schematic representation of the electronic movement in the ring 'a' and 'b' which are closed by intramolecular hydrogen bonds.

model 11

model 21

model 12

model 22

model 13

model 23
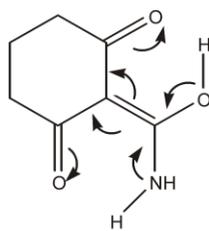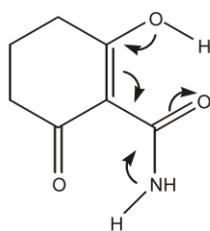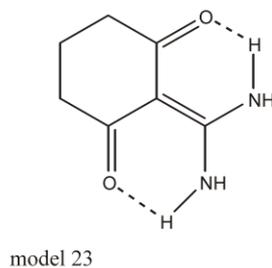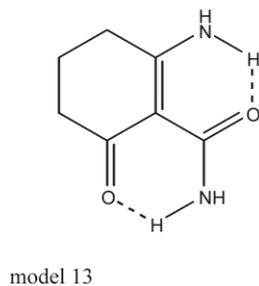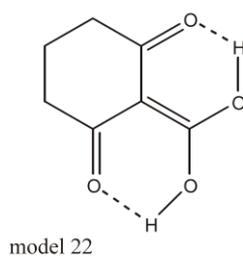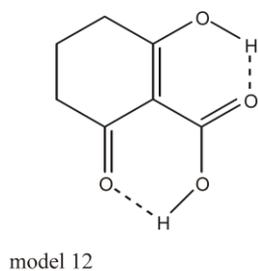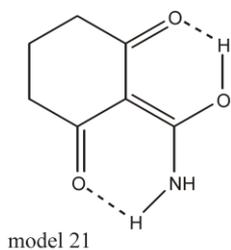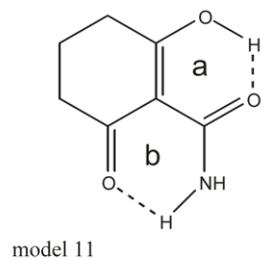
Table 5. Geometrical (Å, °) and topological (ρ in e/Å^3 and $\nabla^2\rho$ in e/Å^5) parameters of the intramolecular hydrogen bonds of the optimized

models. Hydrogen-bonding energies are calculated according to Espinosa [34] ($E = 25.3 \times 10^3 e^{-3.6(H...A)}$) and $E_{HB} = \frac{1}{2} V(\mathbf{r}_{BCP})$ (in kcal/mol)

with local energy densities G, V, H (in a.u.).

	D-H	H...A	D...A	<D-H…A	ρ(H...A)	$\nabla^2\rho$	E_{HB}geom	E_{HB}	G	V	H	V/G
O-H…O												
model 11a	1.00	1.50	2.457	152	0.53	3.1	-27.25	-27.98	0.0640	-0.0892	-0.0252	1.39
model 12a	1.00	1.56	2.499	150	0.44	3.5	-21.68	-22.61	0.0548	-0.0721	-0.0172	1.31
model 12b	1.01	1.66	2.576	150	0.35	3.1	-15.27	-16.43	0.0439	-0.0524	-0.0085	1.19
model 21a	1.00	1.48	2.451	153	0.55	3.3	-29.21	-29.80	0.0660	-0.0950	-0.0290	1.43
model 22a	1.01	1.55	2.500	151	0.44	4.4	-22.58	-23.45	0.0556	-0.0747	-0.0192	1.34
model 22b	1.00	1.55	2.500	151	0.44	4.4	-22.62	-23.49	0.0556	-0.0749	-0.0192	1.34
N-H…O												
model 11b	1.02	1.89	2.68	132	0.19	3.1	-6.82	-8.19	0.0276	-0.0261	0.0015	1.05
model 13a	1.02	1.75	2.57	134	0.27	3.9	-11.08	-12.72	0.0386	-0.0406	-0.0019	1.05
model 13b	1.02	1.84	2.64	133	0.22	3.4	-7.92	-9.41	0.0310	-0.0300	0.0010	0.97
model 21b	1.02	1.84	2.64	132	0.22	3.4	-7.92	-9.34	0.0304	-0.0298	0.0006	0.98
model 23a	1.02	1.74	2.58	136	0.27	4.3	-11.43	-13.034	0.0390	-0.0416	-0.0026	1.06
model 23b	1.02	1.74	2.58	136	0.27	4.3	-11.34	-12.96	0.0388	-0.0413	-0.0025	1.06

In all cases the estimated binding energies obtained from the energy densities are comparable with those calculated from distance-dependent relations [34] (Table 1 and Table 5). The values are sensitive against the hydrogen bond types involved and against the molecular symmetry. The following trends are observed: O-H...O contacts have generally larger energy values (-16 to -30 kcal/mol) than N-H...O contacts (-8 to -13 kcal/mol). The values reach their maximum for O-H...O and their minimum for N-H...O when both bond types appear together (models 11 and 21). The O-H...O bond energy is significantly weaker if another competing O-H...O contact is exhibited in the structure (compare models 21 and 22). The effect of the molecular symmetry becomes visible if one compares model 12 with 22 and 13 with 23. For higher symmetries higher hydrogen bond energies are found.

Additionally, an interaction may be classified by the ratio of the potential to the kinetic energy density at the bcp ($|V(\mathbf{r}_{bcp})|/G(\mathbf{r}_{bcp})$). Espinosa and co-workers [35] have identified a 'transit region' between covalent and 'pure closed shell' interactions, for which $1 < |V(\mathbf{r}_{bcp})|/G(\mathbf{r}_{bcp}) < 2$. $|V(\mathbf{r}_{bcp})|/G(\mathbf{r}_{bcp}) > 2$ is characteristic for covalent interactions, while $|V(\mathbf{r}_{bcp})|/G(\mathbf{r}_{bcp}) < 1$ defines pure closed shell interactions. It was found that $|V(\mathbf{r}_{bcp})|/G(\mathbf{r}_{bcp})$ is >1 for all O-H…O hydrogen bonds and a few N-H…O hydrogen bonds (model 13, 23) which places them in the 'transit region' of partially covalent interactions. The remaining N-H…O hydrogen bonds, are pure closed shell interactions, with $|V(\mathbf{r}_{bcp})|/G(\mathbf{r}_{bcp}) < 1$.

2.6.   *The source function in H-bonded systems.*

The source function (SF) introduced by Bader and Gatti [11], which was recently reviewed and amply discussed allows for a classification of hydrogen bonds [36, 37]. The potential applications of the SF are, however not fully explored. Very recently Farrugia and Macchi [38] have claimed that π-electron delocalization is not noticeable in the SF contribution, when

reference point is located in the nodal plane of π-distribution. However, σ and π-distributions are self-consistently interrelated and small effect of electron conjugation is revealed, when the reference point lies in the nodal plane. Results based on conjugated hydrocarbons systems presented by Gatti [39] confirmed that π-distribution has an indirect effect on the σ density. The SF describes the contribution of the local sources (LS, single atoms) to the electron density at bond critical point (bcp) of the hydrogen bond. The integrated source contributions from the H atoms supports the Gilli characterization scheme [14, 36, 37, 40]. In particular types of hydrogen bonds the contributions from the hydrogen atom S(H), the donor atom S(D) and the acceptor atom S(A) are as follows:

- **IHB** (isolated hydrogen bond): S(H)% is highly negative and less than -70%, S(D) is very high and >> S(A) and S(D+H+A) amounts $\approx$ 50%, what is consistent with their electrostatic nature;

- **PAHB** (polarization-assisted hydrogen bond): S(H) is halved in percentage with respect to **IHB**, S(D) is less than twice S(A), and S(D+H+A) $\approx$ 70%;

- **RAHBs** (resonance assisted hydrogen bond): have very small but positive S(H), comparable source contributions S(D) $\approx$ S(A) and S(D+H+A) $\approx$ 70%, S(H+A)% $\approx$ 35%,

- **±CAHBs** (charge assisted hydrogen bond): are characterized by S(H) $\approx$ 30%, S(D) amounts to 1/5 S(A), S(D+H+A) > 90 %, S(H+A) > 80%, what is consistently with a localized and nearly covalent nature [36, 37, 40].

The attraction of this method is that the source function can in general be obtained both from experimental and theoretical charge densities. Recently we proved the existence of a N-H...O resonance assisted hydrogen bond by analysis of an experimental charge density [4]. Since the experimental charge density distribution is not available in the present case a

classification based on theoretical calculations was used. The results for the hbs in all model species are presented in Table 6. For the title compound and model 11 the contribution of the H, D, and A atoms are comparable as expected. For the intramolecular O-H…O hydrogen bonds in all presented models the characteristic features reported for RAHBs are well reproduced, that means a small but positive source contribution of the H atoms, and also high contributions are observed for atoms comprising the S (D+H+A). Model 12 is an exception, here a negative H-atom contribution is found for the contact of ring 'b' with a concomitantly large S(D) values which points towards an polarization-assisted hydrogen bond. This tendency is reflected in the geometric parameters of the six H-bonded b-rings (also for the symmetrical models 22 and 23), which suggests that these hydrogen bonds are rather isolated than resonance assisted, which is in line with the lack of a conjugated system in ring 'b'. For the intramolecular N-H…O bonds negative source contributions are observed for the donating H atoms (S(H)= -6.9% to -16.9%) and the combined (D+H+A)-contributions constitute in the range of 37.9%-53.3% indicating that these are neither pure isolated, nor polarization-assisted hydrogen bonds. The results for model 23 seem to be counterintuitive because two intramolecular resonance-assisted hydrogen bonds are expected there.

This can be explained by the fact that a classification of HBs, according to Gatti's work [37] is generally based on systems containing O-atoms. However, Gatti also examined systems with other donor and acceptor atoms, like N, C, F, simultaneously broadening the spectrum of hydrogen bonds to low- barrier hydrogen bonds (LBHB) and short-strong hydrogen bond (SSHB). However, studies addressing hydrogen bonds in terms of source function have been more applied to O-H…O hydrogen bonds [15, 42-44] than to N-H…O hydrogen bonds [42, 45]. Nevertheless it is worth mentioning that a negative S(H) values is observed for weak N-H…O hydrogen bonds [41, 44]. These results confirm the lower degree of delocalization in ring 'b' for the less symmetrical models 11-13 and 21.

Table 6. Integrated source contributions of all optimized models (given in percent).

	S(H)	S(D)	S(A)	S(H+A)	S(H+D)	S(D+H+A)
O-H...O						
model 11a	11.3	26.3	35.6	46.9	37.6	73.2
model 12a	2.2	33.9	32.5	34.7	36.1	68.6
model 12b	-7.9	41.5	28.2	20.3	33.6	61.8
model 21a	9.5	27.2	36.4	45.9	36.8	73.2
model 22a	4.9	32.5	32.8	37.7	37.3	70.2
model 22b	2.5	32.4	33.3	35.8	35.0	68.3
form B_opt	8.2	29.4	34.5	42.7	37.6	72.0
N-H...O						
model 11b	-16.5	36.6	17.8	1.3	20.1	37.9
model 13a	-7.4	33.6	25.4	18.0	26.3	51.7
model 13b	-13.6	36.3	20.8	7.2	22.7	43.5
model 21a	-12.1	35.6	21.6	9.4	23.5	45.1
model 23a	-8.1	34.3	26.1	17.9	26.2	52.2
model 23b	-6.9	34.6	25.6	18.7	27.7	53.3
form B_opt	-16.9	37.3	18.1	1.2	20.4	38.5

2.3.   Electron Localizability Indicator and Delocalization Index

In order to elucidate the detailed electron distribution of the model compounds the Electron Localizability Indicator [10] is analyzed. Moreover, the delocalization index [12, 45] has been applied which quantifies electron sharing along specific 1,2- and 1,3-contacts. In Figure 3 the AIM bond paths and bond critical points and the ELI-D localization domains are given for model 11. See supporting information for all models.

In all models the integrated electron populations of the six electron pair basins constituting the six-membered rings 'a' and 'b' (including the protonated valence basin $V_1(H,O/N)$ and the "unbound" electron pair of the O-atom which points towards the H-atom) indicate resonance effects since they don't follow any possible single-double-single-double

scheme which would be drawn by chemists, but show a quite equally distributed electron density (see supporting information for full lists, Tables S1-S7). The aliphatic C-C bonds of ring 'c' vary in the range from ca. 1.9-2.1 e in the six models, whereas the C-C bonding basins of rings 'a' and 'b' carry 2.3-2.7 e. Concomitantly, all C-N and C-O bonds lie between the expected values for single and double bonds [47]. An exception is the d3a bond in models 11-13 with the large electron population of ca. 3.3 e which confirms the results above.

It is interesting to note that the electron pairs of the unbound valence basins of the O-atoms are asymmetrically distributed since a significantly lower amount of electrons is located in the basin involved in the intra-molecular hydrogen bond. For those models including O-H...O and N-H...O contacts, this asymmetry is always larger for O-H...O contacts (2.5 e vs. 3.0 e) than for N-H...O contacts (2.6 e vs. 2.8 e). Moreover, the shift of electrons from the formal C=O double bond to the unbound electron pairs is always a little bit larger in case of O-H...O=C; C=O (O-H...O) ca. 2.0 e, C=O (N-H...O) ca. 2.2 e. Therefore, it seems that resonance effects are more pronounced for the rings including O-H...O contacts. This may be due to the fact, that O-atoms have two basins of unbound electron pairs, which permits a larger range of electron movements since electrons could also be shifted between the two unbound electron pairs. For the two H-atoms of the amide fragment the situation is opposite to the unbound electron pairs of the O-atoms. Here, the protonated valence basin which is involved in the N-H...O contact (2.1 e) carries more electrons than the other one (2.0 e).

A detailed analysis of models 11-13 reveals that, as expected, resonance effects are more pronounced within ring 'a' than within ring 'b'. To exemplify this, we focus on the unbound electron pairs of the N and O atoms and the corresponding C-O, C=O, and C-N bonds. For all R-O-H and R-NH$_2$ fragments, the electron population of the unbound electron pairs is smaller if those atoms are located in ring 'a' as they supply density to the corresponding C-O and C-N single bonds. For the keto-functions, the situation is opposite: the

unbound valence electrons of those O-atoms which are located in ring 'a' carry more electrons than those of ring 'b'. Accordingly, the C=O bonds are always less populated in ring 'a' than in ring 'b'. Since the d3a bond still has basically double bond character, both mesomeric forms of ring 'a' are obviously not equipollent. In models 21-23 two rings compete for resonance. Accordingly, the corresponding electron numbers in terms of ELI-partitioning are almost all in between those of ring a and ring b of models 11-13.

The results are confirmed by the delocalization index (see supporting information for full lists, Tables S8-S13). The values for the 1,2-contacts follow the same trend as the ELI-populations of the disynaptic valence basins. Here, we focus on the 1,3-contacts to investigate its usefulness for determination of resonance effects. For clearance, only model 11 (which refers to the title compound) will be discussed in detail. $\delta_{1,3}(C,C)$ is about 0.05 for the C-atoms in the aliphatic part. For the three C-atoms within ring 'a' it increases to 0.06, but for the three C-atoms within ring 'b' it is 0.04. However, the differences are quite small so that resonance effects are not clearly visible. For 1,3 N/O-C-C contacts, the values range from 0.09 to 0.15, and for the N-C-O acid amid part it is as large as 0.27, but it is not clear whether this is related to a higher degree of resonance along those bonds or if these results are just a consequence of the different atom types involved.
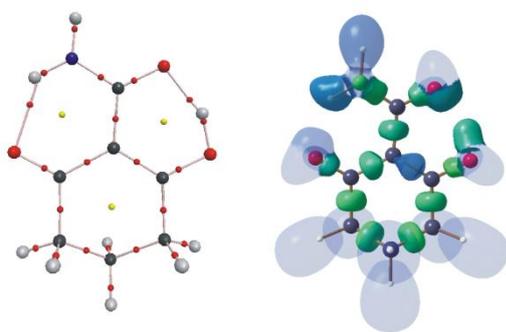
Figure 3 Theoretical AIM-topology (left) and ELI-D distribution in model 11. In the latter one, the basins are double coded for clarity with respect to their sizes: small basins are green and solid whereas large basins are increasingly blue and transparent. One finds the d3a bond (C5-C10) to be significantly larger which reflects its double-bond character. The electronic effects of two intramolecular hydrogen bonds are clearly visible.

Having this in mind, the 1,2- and 1,3-contacts involving the intramolecular hydrogen bonds are briefly discussed. For N-H...O $\delta_{1,2}(H,O)$ and $\delta_{1,3}(N,O)$ are 0.09 and 0.08, whereas larger values are found for O-H...O ($\delta_{1,2}(H,O) = 0.17$, $\delta_{1,3}(O,O) = 0.15$). If one analyzes model 12 which contains two O-H...O contacts, one finds slightly larger electron sharing along the hydrogen bond in ring a ($\delta_{1,2}(H,O) = 0.15$, $\delta_{1,3}(O,O) = 0.14$) than in ring b ($\delta_{1,2}(H,O) = 0.13$, $\delta_{1,3}(O,O) = 0.11$). So like for the C-C bonds resonance effects are indeed visible but the quantitative differences are nevertheless very small and one always have to consider the atomic species involved.

3. Experimental

3.1. Materials and methods

Compound (I) was synthesized as described in the literature [5]. This compound is both a product of the reaction of potassium cyanate with dimedon and the substrate in reactions with 1,2-phenylenediamines [48]. The crystal structure was presented by Tonkikh and coworkers [48].

Very thin single crystals were obtained by recrystallization of compound (I) by slow evaporation from a toluene solution, so we used synchrotron radiation for adequate intensities. Although the crystal quality was limited, high quality diffraction data for a single crystal with

dimensions 0.02 x 0.02 x 0.05 mm could be collected. Data collection was done at the F1 beamline at HASYLAB/DESY (Hamburg) applying a Huber 4-circle diffractometer and a MARCCD 165 area detector. Integration, data reduction and scaling were done using the XDS package (version 2009 [49]). The structure was solved with *SHELXS*[50] and refinement was carried out using *SHELXL97*[50]. Further details are presented in Table 6.

Table 6   Crystal data and structure refinement for compound (I) at 100K.

	compound I
Empirical formula	$C_9H_{13}N_1O_3$
Molecular weight [g/mol]	183.20
Crystal description	block, light yellow
size [mm]	0.02 x 0.02 x 0.05
Crystal system	monoclinic
Space group	P 2_1/c
a [Å]	12.136(1)
b [Å]	6.580(1)

c [Å]	13.601(1)
β [º]	120.64(1)
V [Å^3]	934.8(2)
Z	4
d_x [g cm^{-3}]	1.302
µ [cm^{-1}]	0.043
F(000)	392
λ [Å]	0.5000(3)
max θ [°]	42.0
sin θ/λ [Å^{-1}]	1.12
No. of measured reflns	21473
No. of unique reflections	1567
$R_{(int)}$	0.019
No. of observed reflns (I>2 σ(I))	1480
restraints/parameters	0/132
Goodness-of-fit on F^2	1.07
wR_2(obs)/ wR_2(all)	0.0892/0.0874
wR_1(obs)/ wR_1(all)	0.0365/0.0345
$\Delta\rho_{min}/\Delta\rho_{max}$ [e/Å^3]	-0.19/0.26

3.2. Computational details

Theoretical calculations were performed at the B3LYP/6-311++G** level of theory [51] using GAUSSIAN03 [52]. For all models frequency calculations were carried out to check that all optimized geometries correspond to energy minima. A large variety of theoretical calculations was performed:

Single Point (SP) calculations based on the structural geometry of the molecule and for a dimer generated by a center of inversion,

all possible tautomers of 2-hydroxy-4,4-dimethyl-6-oxo-cyclohex-1-ene carboxy amide (called forms A, B, and C) were fully optimized in order to estimate the energy differences between them (see scheme 1),

full geometry optimization was done for the dimer (dimer_opt, see figure 2).

Six smaller models (11-13, 21-23) with two adjacent intramolecular hydrogen bonds were optimized (scheme 3). Models 11-13 and 21-23 are without methyl groups, which are equivalent to H atoms in the substituent effect, and are not important for hydrogen bonds [53].

For all six models and the title compound theoretical structure factors were generated from the wave function files using TONTO [54]. Refinement against the theoretical structure factors by XD2006 [55], led to theoretical multipole models of the gas phase structures. For these models the source function (SF) was determined using the XDPROP module of XD Finally, the wave functions were analyzed with AIM2000 [56] and DGRID [57] in order to obtain the delocalization index and the ELI-D.

4. Conclusion

The present study of two intramolecular hydrogen bonds is based on the one hand on the analysis of the geometric parameters obtained from an X-ray experiment (compound I) compared to structures found in the CSD data base, on the other hand on supporting DFT calculations. The results confirm that 2-hydroxy-4,4-dimethyl-6-oxo-cyclohex-1-ene carboxy

amide is the most stable tautomer (form B) in the solid state and in the gas phase. Ab initio calculations give relative energy values which show an agreement with structural data and indicate that forms A and C of the tautomeric mixture are exceptionally little populated ($<10^{-10}$ %). The tautomeric form B is stabilized by two intramolecular hydrogen bonds: O-H...O (medium strength) and N-H...O (weak hydrogen bond). The real-space bonding descriptors of those interactions were analyzed, which are being expected resonance assisted (O-H...O) and isolated (N-H...O). Therefore optimized structures of smaller models were considered and analyzed with the Electron Localizability Indicator and the delocalization index. Generally, the resonance effects are more pronounced within ring 'a' than within ring 'b', which means that delocalization effects are mostly visible in a O=C-C=C-O-H conjugated system. Despite the fact that for models 21-23 one might expect a resonance in both rings, the source contribution analysis confirmed it only for model 22. In terms of the integrated source contribution of the H atom the N-H…O hydrogen bond within ring 'b' may be classified to be between pure isolated and polarization-assisted. The topological and energetic analysis revealed partially covalent character for all O-H…O hydrogen bonds and for the N-H…O hydrogen bonds in models 13 and 23. Therefore the hydrogen bonds were classified as being of medium strength, which is confirmed by the estimated energies for these hydrogen bonds.

Acknowledgements

References

[1]   B. Kuhn, P. Mohr, M. Stahl, M. *J. Med. Chem.*, 2010, **53**, 2601-2611.

[2]   M. Małecka, *Struct Chem.*, 2010, **21**, 175–184.

[3]   M. Małecka, *J. Mol. Struct.,* 2007, **831**, 135-143.

[4]   M. Małecka, L. Chęcińska, A. Rybarczyk-Pirek, W. Morgenroth, C. Paulmann, *Acta Cryst.,* 2010, **B66**, 687–695.

[5]   H. Muxfeld, G. Grethe, W. Rogalski, *J. Org. Chem.*, 1966, **31**, 429–2430.

[6]   G. Bertolini, M. Aquino, M. Biffi, G. d'Arti, F. Di Pierro, F. Ferarrio, P. Mascagni, F. Somenzi, A. Zaliani, F. Leoni, *J.Med. Chem.*, 1997, **40**, 2011-2016.

[7]   T. H. Kim, H-S. Na, H-S, M. Loffler, *Arch. Pharm. Res.,* 2003, **26**, 197-201.

[8]   M. T. Cocco, C. Congiu, V. Lilliu, V. Onnis, *Arch. Pharm.*, 2006, **339**, 7 – 13.

[9]   R. F. W. Bader, *Atoms in Molecules. A Quantum Theory*. Oxford University Press. **1990**

[10] M. Kohout, *Int. J. Quantum Chem,* 2004, **97**, 651–658.

[11] R. F. W. Bader, C. Gatti, *Chem. Phys. Lett.,* 1998, **287**, 233–238.

[12] R. F. W. Bader; M. E. Stephens, .*J. Am. Chem. Soc.,* 1975, **97**, 7391–7399.

[13] D. Cremer, J. A. Pople, *J. Am. Chem. Soc.*, 1975, **97**, 1354-1358.

[14] P. Gilli, F. Bellucci, V. Ferretti, V. G. Bertolasi, *J. Am. Chem. Soc.*, 1989, **111**, 1023–1028.

[15] T. Steiner, *Angew. Chem. Int. Ed.*, 2002, **41**, 48-76.

[16] M. C. Etter, *Acc. Chem. Res.*, 1990, **23**, 120–125.

[17] P. Kollat, J. J. Stezowski, *Acta Cryst.*, 1982, **B38**, 2531-2533.

[18] J. V. Silverton, C. Kabuto, T. Akiyama, *Acta Cryst.*, 1982, **B38**, 3032-3037.

[19] G. J. Palenik, M. Mathew, R. Restivo, *J. Am. Chem. Soc.*, 1978, **100**, 4458-4464.

[20] W. Clegg, S. J. Teat, *Acta Cryst.*, 2000, **C56**, 1343-1345.

[21] R. Martos-Calvente, V. A. de la Pena O'Shea, J. M. Campos-Marti, J. L.G. Fierro, *J. Phys. Chem.*, 2003, **A107**, 7490-7495.

[22] N. Campillo, C. Montero, J. A. Paez, *J. Mol. Struct.*, *(THEOCHEM)*, 2004, **678**, 83-89.

[23] F. H. Allen, O. Kennard, D. G. Watson, L. Brammer, A. G. Orpen, R. Taylor, *International Tables for X-ray Crystallography*, 1992, **Vol. C, ch. 9.5**, 685–706. Amsterdam: Kluwer Academic Publishers.

[24] Cambridge Crystallographic Data Centre 2011. ConQuest, Version 1.13. CCDC, 12 Union Road, Cambridge, UK; http://www.ccdc.cam.ac.uk/products/csd_system/.

[25] V. Bertolasi, P. Gilli, G. Gilli, *J. Am. Chem. Soc.*, 1991, **113**, 4917-4925.

[26] S. J. Grabowski, *J. Phys. Chem.,* 2001, **A105***, 10739-10746.

[27] S. J Grabowski, *J. Mol. Struct.*, 2002, **615**, 239–245.

[28] J. E. Del Bene, I. Alkorta, J. Elguero. *J. Phys. Chem.,* 2010, **A114**, 49, 2958-12962.

[29] H. Szatyłowicz, T. M. Krygowski, A. Jezierska-Mazzarello, *J. Mol. Model.,* 2011, **17***, 125-131.

[30] P. Popelier, *Atoms in Molecules*. An introduction, Prentice Hall, Harlow 2000.

[31] U. Koch, P. L. A. Popelier, *J. Phys. Chem.*, 1995, **99**, 9747–9754.

[32] I. Rozas, I. Alkorta, J. Elguero, *J. Am. Chem. Soc.*, 2000, **122**, 11154–11161.

[33] D. Cremer, E. Kraka, *Angew. Chem.*, Int. Ed. Engl. 1984, **23**, 627-628.

[34] E. Espinosa, E. Molins, C. Lecomte, *Chem. Phys. Chem.*, 1998, **285**, 170–173.

[35] E. Espinosa, I. Alkorta, J. Elguero, E. Molins, *J. Chem. Phys.*, 2002, **117**, 5529-5542.

[36] C. Gatti, F. Cargnoni, L. Bertini, *J. Comput. Chem.*, 2003, **24**, 422–436.

[37] C.Gatti, *Struct. & Bond.*, *The Source Function Descriptors as a Tool to Extract Chemical Information from Theoretical and Experimental Electron Densities*, 2012, **147**, 193-286.

[38] L. J. Farrugia, P. Macchi, *J. Phys. Chem.,* 2009*, **A113***, 10058-10067.

[39] E. Monza, C. Gatti, L. L. Presti, E. Ortoleva, *J. Phys. Chem.,* 2011*, **A115***, 12846-12878.

[40] G. Gilli, P. Gilli, *J. Mol. Struct*., 2000*, **552***, 1-15.

[41] G. A. Jeffrey, An Introduction to Hydrogen Bonding; Oxford University, Press: New York, 1997.

[42] J. Overgaard, B. Schiøtt, F. K. Larsen, B. B. Iversen, *Chem. Eur. J.,* 2001, **7**, 3756–3767.

[43] D.E. Hibbs, J. Overgaard, R. O. Piltz, *Org. Biomol. Chem.,* 2003, **1**, 1191–1198.

[44] J. Sørensen, H. F. Clausen, R. D. Poulsen, J. Overgaard, B. Schiøtt, *J. Phys. Chem.,* 2007, **A111**, 345–351.

[45] M. Schmidtmann, L. J. Farrugia, D. S. Middlemiss, M. J. Gutmann, G. J.; McIntyre, C. C. Wilson, *J. Phys. Chem.,* 2009*, **A113***, 13985–13997.

[46] X. Fradera, M. A. Austen, R. F. W. Bader, *J. Phys. Chem.,* 1999, **A103**, 304-314.

[47] S. Mebs, PhD Thesis, Freie Universität Berlin, 2009.

[48] N. Tonkikh, A. Strakovs, M. Petrova, V. V. Chernyshev, H. Schenk, *Chem. Heterocycl. Comp.,* 2002*, **38***, 724-729*.

[49] W. Kabsch, *J. Appl. Cryst*. 1993, **26**, 795–800.

[50] G. M. Sheldrick, *Acta Cryst.* 2008, **A64**, 112–122.

[51] A. D. Becke, *Phys. Rev.,* 1988, **A38**, 3098-3100.

[52] M.J. Frisch, G.W. Trucks, H.B. Schlegel, G.E. Scuseria, M.A. Robb, J.R. Cheeseman, J.A. Montgomery Jr., T. Vreven, K.N. Kudin, J.C. Burant, J.M. Millam, S.S. Iyengar, J. Tomasi, V. Barone, B. Mennucci, M. Cossi, G. Scalmani, N. Rega, G.A. Petersson, H. Nakatsuji, M. Hada, M. Ehara, K. Toyota, R. Fukuda, J. Hasegawa, M. Ishida, T. Nakajima, Y. Honda, O. Kitao, H. Nakai, M. Klene, X. Li, J.E. Knox, H.P. Hratchian, J.B. Cross, C. Adamo, J. Jaramillo, R. Gomperts, R.E. Stratmann, O. Yazyev, A.J. Austin, R. Cammi, C. Pomelli, J.W. Ochterski, P.Y. Ayala, K. Morokuma, G.A. Voth,

P. Salvador, J.J. Dannenberg, V.G. Zakrzewski, S. Dapprich, A.D. Daniels, M.C. Strain, O. Farkas, D.K. Malick, A.D. Rabuck, K. Raghavachari, J.B. Foresman, J.V. Ortiz, Q. Cui, A.G. Baboul, S. Clifford, J. Cioslowski, B.B. Stefanov, G. Liu, A. Liashenko, P. Piskorz, I. Komaromi, R.L. Martin, D.J. Fox, T. Keith, M.A. Al- Laham, C.Y. Peng, A. Nanayakkara, M. Challacombe, P.M.W. Gill, B. Johnson, W. Chen, M.W. Wong, C. Gonzalez, J.A. Pople, *Gaussian 03*, revision C.02; Gaussian, Inc. Wallingford, CT, 2004.

[53] C. Hansch, A. Leo, R. W. Taft, *Chem.Rev.*, 1991, **91**, 165-195.

[54] D. Jayatilaka, D. J. Grimwood, TONTO: *A Fortran Based Object-Oriented System for Quantum Chemistry and Crystallography, UserManual*: The University of Western Australia, Perth, Australia, 2003.

[55] T. Koritsánszky, P. R. Mallinson, P. Macchi, A. Volkov, C. Gatti, T. Richter, L. J. Farrugia, XD2006, A Computer Program package for Multipole Refinement, Topological Analysis of Charge Densities and Evaluation of Intermolecular Energies from Experimental or Theoretical Structure Factors . Program Version 5.33, User Manual 2007.

[56] F. Biegler-König, AIM2000 program, University of Applied Sciences, Bielefeld, Germany, 2000.

[57] M. Kohout, *DGrid and Basin*, version 4.4; Max-Planck-Institut für Chemische Physik fester Stoffe: Dresden, Germany, 2009.